Heliyon 10 (2024) e38964

Contents lists available at ScienceDirect

Heliyon

journal homepage: www.cell.com/heliyon

Research article

Exploring the role of endoplasmic reticulum stress in recurrent spontaneous abortion: Identification of diagnostic biomarkers and immune cell interactions

Tao Tang [a,1], Jingyu Fu [b,1], Chong Zhang [c,1], Xue Wang [d], Haiming Cao [e,f,**], Lin Chen [d,*]

[a] Department of Orthopedic Surgery, The Second Affiliated Hospital of Anhui Medical University, Hefei, China
[b] Department of General Surgery, Lu'an Hospital of Anhui Medical University, Lu'an, China
[c] Department of General Surgery, Jinshan Hospital Affiliated to Fudan University, Shanghai, China
[d] Department of Ophthalmology, The Second Affiliated Hospital of Anhui Medical University, Hefei, China
[e] Department of Urology, The First Affiliated Hospital of Bengbu Medical University, Bengbu, China
[f] Center for Reproductive Medicine, The Seventh Affiliated Hospital of Sun Yat-sen University, Shenzhen, China

ARTICLE INFO

Keywords:
Endoplasmic reticulum stress
Recurrent spontaneous abortion
Immune response
Bioinformatics
Immune cell infiltration

ABSTRACT

Dysregulated endoplasmic reticulum stress (ERS) is associated with recurrent spontaneous abortion (RSA) and is involved in the mechanisms that govern immune balance and vascular regulation at the maternal-fetal interface. The molecular intricacies of these mechanisms remain elusive. This study employed microarray and bioinformatics techniques to examine genetic abnormalities in endometrial tissues from RSA patients, with the objective of identifying potential ERS-related biomarkers. By integrating two publicly available microarray datasets, consisting of 88 RSA and 42 control samples, we conducted an extensive analysis, including differential expression, functional annotation, molecular interactions, and immune cell infiltration. Analysis of immune cell characteristics suggests an inflammatory immune imbalance as a potential contributor to RSA progression. Both innate and adaptive immunity were found to play roles in RSA development, with M1 macrophages constituting a significant proportion of immune infiltration. We identified five key ERS-associated genes (TMEM33, QRICH1, MBTPS2, ERN1, and BAK1) linked to immune-related mechanisms, with RT-qPCR results aligning with bioinformatics findings. Our research findings offer a fresh and comprehensive perspective on the ERS-related genes' pathways and interaction networks, offering significant insights for the advancement of innovative therapy techniques for RSA.

1. Introduction

The unfortunate occurrence of two or more consecutive pregnancy losses, referred to as recurrent spontaneous abortion (RSA), represents a heartbreaking challenge for couples aspiring to become parents [1,2]. Despite extensive research into its etiology, a

* Corresponding author. The Second Affiliated Hospital of Anhui Medical University, Hefei, 230000, China.
** Corresponding author. The First Affiliated Hospital of Bengbu Medical University, Bengbu, 233000, China.
E-mail addresses: caohm3@mail2.sysu.edu.cn (H. Cao), cltt107428@126.com (L. Chen).
[1] Each of these writers made an equal contribution to this work and ought to be regarded as co-first authors.

https://doi.org/10.1016/j.heliyon.2024.e38964
Received 3 January 2024; Received in revised form 2 October 2024; Accepted 3 October 2024
Available online 5 October 2024

substantial proportion of RSA cases remain unexplained, resulting in the categorization of unexplained recurrent spontaneous abortion (URSA) [3,4]. This condition causes considerable physical and emotional distress and highlights the urgent need to explore new avenues in reproductive medicine.

The endoplasmic reticulum stress (ERS) pathway has come to light as a potentially important element in the context of RSA due to recent breakthroughs in our understanding of cellular stress responses. The endoplasmic reticulum, a complex cellular organelle, is responsible for critical processes such as protein and lipid synthesis, calcium homeostasis, and protein folding [5]. ERS, initiated by disturbances in endoplasmic reticulum homeostasis and governed by the unfolded protein response (UPR), has emerged as a significant contributor to numerous cellular functions [6]. Intriguingly, recent investigations have elucidated the complex role of ERS in human fertility [7], with several ERS-related genes and proteins showing elevated expression during embryo implantation [8], thus implicating ERS in this fundamental reproductive event [9].

ERS has been identified as a key modulator of uterine apoptosis and homeostasis [10], indicating its potential role in recurrent pregnancy loss [11,12]. Disruptions in ERS responses have been associated with infertility [13,14], and individuals with RSA or repeated implantation failure have endometrial tissue with increased ERS markers [11,15]. Despite these compelling associations, the precise contribution of ERS to RSA remains inadequately understood, and reliable biomarkers for predicting maternal-induced RSA have yet to be identified. Notably, ERS has been shown to influence immune cell behavior and function under various physiological conditions [16–18], suggesting a potential link between ERS and abnormal immune cell infiltration.

Reproductive system abnormalities at the fetal-maternal interface have been linked to changes in the maternal immune response [16,19,20]. ERS, as a regulator of immune cell behavior, may significantly influence the immunological environment at this vital interface [11,21]. Furthermore, aberrant immune cell responses are known to contribute to embryo rejection, implantation failure, and recurrent miscarriage [22]. Consequently, knowledge of the relationship between the ERS and the infiltration of immune cells at the mother-fetal interface may reveal crucial new directions on the mysterious processes of RSA.

This study investigates the multifaceted role of ERS in the context of RSA, with a particular emphasis on its interactions with the immune milieu. By delving into the intricacies of ERS and its interplay with the immune system, we aim to shed light on novel diagnostic biomarkers and offer novel perspectives on the pathophysiology of RSA.

2. Methods

2.1. Datasets and data preprocessing

Transcriptome data from endometrial tissues of 88 RSA patients and 42 healthy controls (datasets GSE77688 and GSE141549) were acquired from the Gene Expression Omnibus (GEO) collection. The sva R package's ComBat function was used to rectify batch effects [23]. A training set of 64 patients and 27 controls and a validation set of 24 patients and 15 controls were randomly selected from the dataset in a 7:3 ratio. The workflow and data processing steps are illustrated in Fig. S1.

2.2. Analysis of differential expression and association of ERS genes

The transcriptome data was used to extract 57 ERS genes. The limma R package was used using a linear model technique to identify differentially expressed ERS genes in patients and controls [24]. For the purpose of screening differentially expressed genes (DEGs), the *p*-value threshold was changed to <0.05 and $|\log_2 FC|>1$. Heatmaps and volcano plots produced by the ggplot2 [25] and pheatmap R packages, respectively, were used to display the expression profiles of the differentially expressed ERS genes. For the significantly differently expressed ERS genes, Pearson correlation analysis was performed.

2.3. Proteins, transcription factors, miRNA, small-molecule compound interaction network analysis

A protein-protein interaction (PPI) network was constructed utilizing differentially expressed ERS genes and the Internet Search Tool for the Retrieval of Interacting Genes [26] and Cytoscape software [27]. Interaction networks for transcription factors, miRNAs, and small-molecule compounds were also analyzed. The 15 differentially expressed ERS genes were uploaded to NetworkAnalyst to construct the interaction networks [28]. The databases used included the ENCODE transcription factor database, the Comparative Toxicogenomics Database, and miRTarBase v8.0. Cytoscape software was employed for network visualization.

2.4. Screening candidate diagnostic markers and construction of diagnostic scores

The diagnostic markers were eliminated using regression with the least absolute shrinkage and selection operator (LASSO, Tibshirani) [29]. LASSO is a form of compression estimation that facilitates the development of a more precise model by implementing a penalty function that compresses certain coefficients while nullifying others [30]. The advantages of subset shrinking are maintained by this approach, which also offers a biased estimate method suitable for multicollinear data. The function glmnet from the glmnet R package was employed to select variables, and the combination of identifiers with the least cross-validation (CV) error was chosen [31].

The diagnostic score of each subject was determined by employing the subsequent formula:

$$\text{Diagnostic score} = \sum_{i=1}^{n} \text{Coef}_i \times Exp_i$$

where Coef is the matching Cox regression coefficient and Exp is the gene expression level. Utilizing Maxstat analysis, the diagnostic score's optimal cut-off value for RSA diagnosis was isolated.

2.5. Analysis of differential expression and functional enrichment

DEGs in microarray data were identified using the limma tool in R [24] to compare patient samples with those from control groups. The criteria for screening differentially expressed genes (DEGs) included a significance level of less than 0.05 for the adjusted p-value and a log2 fold change greater than 1 in absolute value. The ggplot2 [25] and pheatmap packages were employed to construct volcano plots and heatmaps, respectively. The clusterProfiler program [32] was used to carry out enrichment studies of the DEGs using Gene Ontology (GO) [33] and Kyoto Encyclopedia of Genes and Genomes (KEGG) [34]. Statistical significance was attained by DEGs with an adjusted *p*-value less than 0.05. Molecular functions (MF), cellular components (CC), and biological processes (BP) are examples of GO functional annotations. Genomics, diseases, medicines, and biological pathways are covered in detail in the extensive database KEGG. Using "c2.cp.kegg.v7.4.symbols.gmt" as the gene set reference and applying a Gaussian distribution for the kcdf parameter, the GSVA approach was utilized to calculate the scores for each gene set [35]. Next, a differential pathway analysis with a *p*-value threshold of less than 0.05 was carried out using the limma R package [24].

2.6. Construction of RSA molecular subtypes

When dealing with datasets like microarray gene expression data, consensus clustering is a method that helps find the ideal number of clusters and members. The principle underlying consensus clustering is that samples extracted from different subclasses of the original dataset should form a new dataset, and clustering results on this new dataset should closely match those of the original dataset in terms of both the number of clusters and the samples within each cluster. If the resulting clusters exhibit stability relative to sampling variation, they are considered to better represent the true subtype structure. The ConsensusClusterPlus R program [36] was utilized to conduct consensus clustering on the DEGs.

In summary, 1000 iterations total—80 % of the samples—were used for clustering. The variations in the area beneath the cumulative distribution function (CDF) curve were evaluated, with the CDF curve's clustering metric being employed to determine the optimal number of clusters. As a result, correlation analyses of the molecular subtypes were carried out using ERS genes linked to diagnostic indicators.

2.7. Analysis of immune cell infiltration

CIBERSORTx was used to assess immune cell infiltration in both cases and controls. To create a matrix for immune cell infiltration, samples were filtered using a $p < 0.05$ threshold. The Wilcoxon test was used to determine the significance of variations in immune cell distribution across different groups. Additionally, we analyzed the correlation between ERS genes associated with diagnostic markers and immune cells.

2.8. Real-time quantitative polymerase chain reaction (RT-qPCR)

The study was authorized by the Seventh Affiliated Hospital of Sun Yat-sen University's Research Ethics Committee (KY-2021-044-01), and all subjects gave written informed consent. RNA extraction from tissues was conducted immediately following the separation of the endometrial tissue of the RSA and control groups, adhering to a previously established methodology. The process began by digesting 150 mg of tissue at 37 °C with an enzyme solution, followed by rapid freezing, mechanical grinding at low temperatures, and homogenization using a tissue disruptor. Total RNA was extracted with TRI Reagent (Invitrogen, USA). To synthesize cDNA, RNA was first quantified using a NanoDrop spectrophotometer (USA), and a specific amount of RNA was then combined with a reaction mix and treated water to prepare a 20 μL reaction mixture. This mixture was subjected to reverse transcription in a PCR machine (Bio-Rad, USA).

RT-qPCR was performed using qPCR Mix (Thermo Fisher Scientific, USA) and a CXF-96 real-time system (Bio-Rad, USA), with the reaction setup containing cDNA, primers, SYBR Green master mix (Thermo Fisher Scientific, USA), and RNase-free ddH2O (Beyotime, China), as outlined in Table S1. Using the 2-ΔΔCt technique and standardization to ACTB, relative gene expression was computed.

2.9. Statistical analysis

The statistical analyses and data computations were carried out utilizing R. Benjamini-Hochberg (BH) adjustments for multiple testing were implemented. The risk of false positives was managed by the use of the false discovery rate (FDR). An independent Student's t-test assessed differences between groups for continuous data following a normal distribution, while the Mann-Whitney *U* test, also known as the Wilcoxon rank-sum test, was applied for non-normally distributed data. ROC curves were plotted, and AUC values were calculated using the pROC R package. In all two-tailed tests, statistical significance was defined by a p-value threshold of

0.05.

3. Results

3.1. Analysis of differential expression and correlation of ERS genes

The expression levels of 57 ERS genes were analyzed between the case and control groups, demonstrating substantial changes in 15 ERS genes. In the case group, it was discovered that TMEM33, QRICH1, MBTPS2, AGR2, NCK1, and BAX were strongly expressed, while ERN1, WFS1, BAK1, KHSRP, EXOSC8, ATF4, EXOSC5, CEBPB, and PPP1R15A showed decreased expression levels (Fig. 1A). The expression profiles of the ERS genes were depicted in a heatmap (Fig. 1B), and a correlation matrix for the ERS genes was created (Fig. 1C).

Correlation coefficients above 0.5 or falling below −0.5 were illustrated with dotted lines (Fig. 2). Positive correlations were observed between CEBPB and PPP1R15A, ATF4 and either CEBPB or PPP1R15A, QRICH1 and BAX, and TMEM33 and NCK1. Conversely, negative correlations were noted between AGR2 and CEBPB, as well as between MBTPS2 and WFS1.

3.2. Analysis of interaction networks for differentially expressed ERS genes

The STRING online database facilitated the selection of 15 ERS genes with differential expression for constructing a PPI network. (Fig. 3A). Interactions were observed among CEBPB, ATF4, PPP1R15A, MBTPS2, NCK1, ERN1, BAK1, BAX, and WFS1, as well as among EXOSC8, KHSRP, and EXOSC5. Transcription factor analysis revealed that ATF4 was associated with 22 transcription factors,

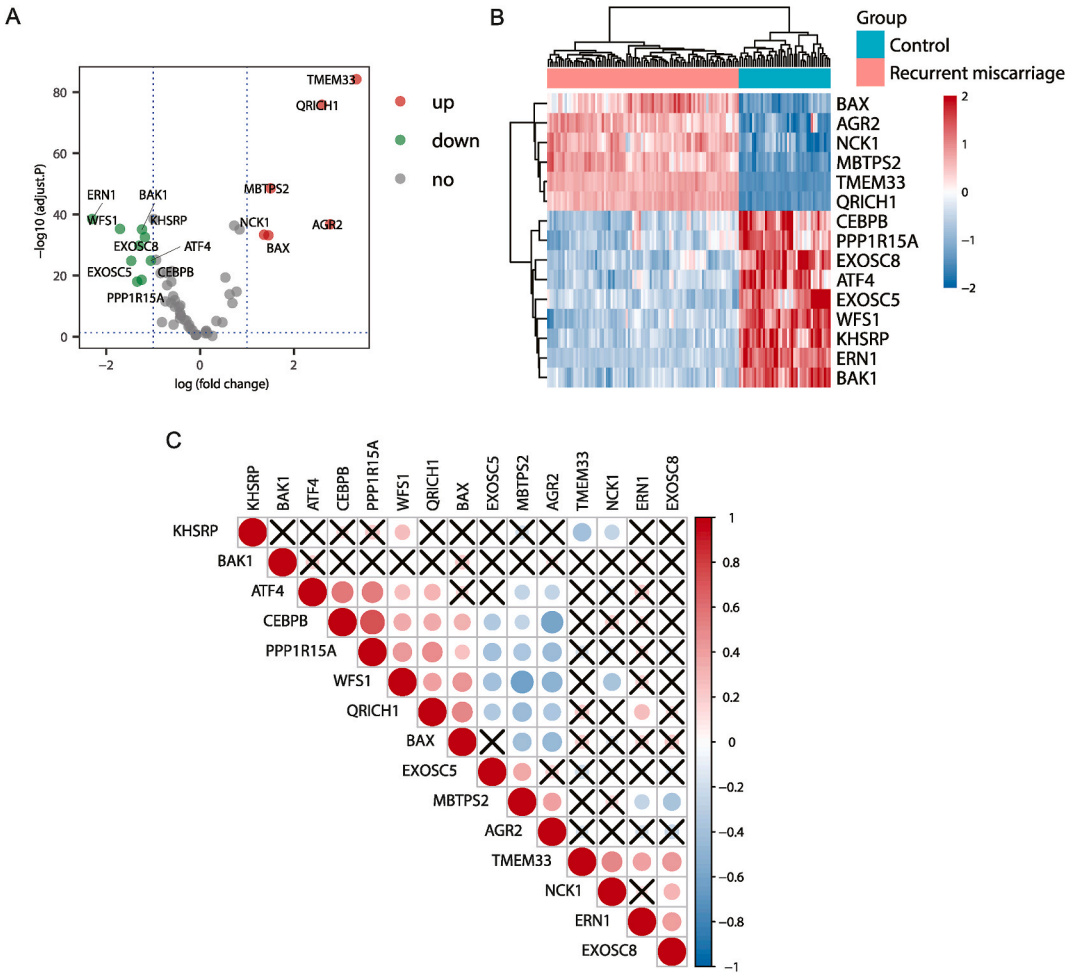

Fig. 1. Expression and correlation analysis of ERS genes. A. ERS genes are expressed differently in cases compared to controls B. Expression levels of ERS genes across samples. C. Correlation matrix depicting the relationships between ERS gene expression levels. The correlation's strength is represented by the color gradient, where stronger correlations are represented by darker colors, Red represents positive correlations, while blue signifies negative ones; Without statistical significance, dark "X" marks are used.

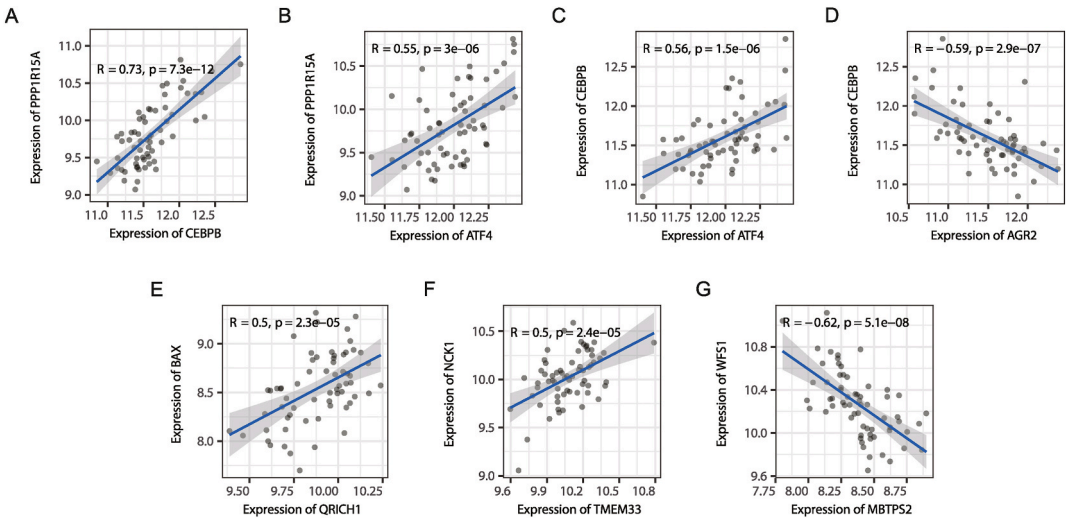

Fig. 2. Pearson correlation analysis of ERS genes. A-G. Significant results from the ERS gene expression levels Pearson correlation analysis.

BAX with 19, PPP1R15A with 17, CEBPB with 16, and BAK1, ERN1, EXOSC5, and QRICH1 with 9 transcription factors each (Fig. 3B). mRNA-miRNA interaction analysis showed that TMEM33 interacted with 9 miRNAs, KHSRP with 7 miRNAs, and CEBPB with 6 miRNAs (Fig. 3C). Small molecule compound analysis revealed that BAX interacted with 23 compounds, CEBPB with 19, PPP1R15A with 16, ATF4 with 14, and ERN1 with 11 compounds (Fig. 3D).

3.3. Screening of ERS markers and validation of differential expression of genes

Five ERS genes were identified as diagnostic markers through LASSO regression analysis: TMEM33, QRICH1, MBTPS2, ERN1, and BAK1 (Fig. 4A and B). The diagnostic score was calculated using the formula: Diagnostic Score = 3.244 × TMEM33 + 1.329 × QRICH1 + (−0.082) × MBTPS2 + 0.238 × ERN1 + (−0.190) × BAK1. The optimal cutoff for this diagnostic score, determined using the maxstat package, was 31.501. The ROC curve for the diagnostic score achieved an AUC of 1, indicating excellent diagnostic performance (Fig. 4C). Scores for both cases and controls are shown (Fig. 4D). Validation of the five ERS markers in the validation set confirmed their differential expression (Fig. 4E). RNA extracted from 24 human endometrial tissues, including 12 from RSA patients and 12 from fertile controls, demonstrated that TMEM33, QRICH1, and MBTPS2 were up-regulated, while ERN1 and BAK1 were down-regulated (Fig. 4F).

3.4. Analyses of functional enrichment and gene expression differences

The expression matrix comprised 2,450 DEGs, including 813 upregulated and 1,637 downregulated mRNAs, as determined through analysis using the limma tool in R. Volcano plots and heatmaps of these DEGs are shown (Fig. 5A and B). Huntington's disease, coronavirus disease, Salmonella infection, ribosome function, and human papillomavirus infection were the pathways in which the DEGs were primarily enriched, according to KEGG pathway analysis (Fig. 5C–F). GO analysis indicated that the DEGs were associated with molecular functions such as binding to protein C-termini and integrins, as well as biological processes including viral transcription, gene expression related to viruses, and cotranslational protein targeting to the membrane dependent on signal recognition particles (SRP) (Fig. 6A and B). GSVA analysis showed that the DEGs were primarily enriched in pathways related to the metabolism of linoleic acid, taurine, hypotaurine, as well as processes associated with mammalian circadian rhythms, glycosylphosphatidylinositol (GPI) anchor production, pantothenate and CoA biosynthesis, and the metabolism of alanine, aspartate, and glutamate. (Fig. 6C and D).

Correlation analysis between differential GSVA pathway scores and ERS gene expression revealed that all differentially expressed ERS genes were correlated with differential GSVA pathway scores (Fig. 6E). In addition to the alanine, aspartate, and glutamate metabolism pathways, QRICH1 showed a substantial positive connection with the taurine and hypotaurine metabolism. Mammals' circadian rhythm pathway and the taurine and hypotaurine metabolism pathway had a strong negative link with MBTPS2, but TMEM33 showed a strong positive correlation.

3.5. Analysis of immune molecule subtypes

To determine consensus molecular subgroups of immune cells, an unsupervised clustering analysis of the DEGs was conducted using the ConsensusClusterPlus R program. The K value was used to calculate the ideal number of clusters. K subtypes were identified from the RSA samples (K = 2–8). Based on the uniformity of the heatmap and the cumulative distribution function (CDF) analysis, four

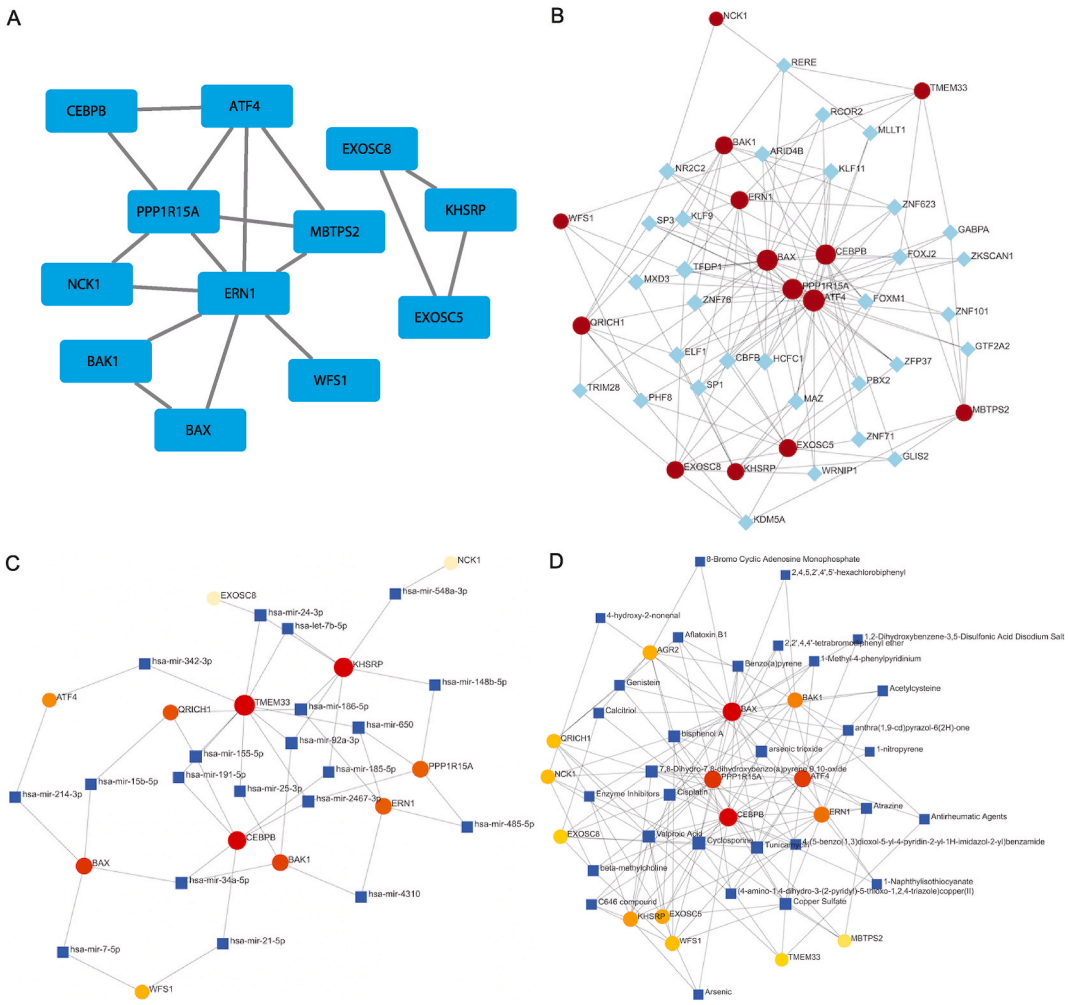

Fig. 3. Interaction network analysis of ERS genes with differential expression A. Depiction of the PPI network highlighting the relationships among differentially expressed ERS genes. B. Visualization of the interaction network connecting these ERS genes to various transcription factors. C. Representation of the interaction network between differentially expressed ERS genes and miRNAs. D. Overview of the interaction network involving differentially expressed ERS genes and small-molecule compounds.

clusters (K = 4) were identified as optimal, suggesting the presence of four distinct molecular patterns, with minimal variation observed in the area of the CDF curve (Fig. 7A–C). Differentially expressed ERS genes were found to be substantially correlated with subtype 1 according to an analysis of correlations between ERS genes and molecular subtypes (Fig. 7D).

3.6. Correlation analysis of immunological microenvironment evaluation and ERS genes

The CIBERSORT algorithm assessed the landscape of 22 different types of infiltrating immune cells, revealing the composition of the immune cell populations (Fig. 8A). RSA and control samples showed variability in immune cell infiltration levels, with principal component analysis (PCA) indicating a significant distinction between the two groups (Fig. 8B). Analysis of correlations between invading immune cells produced an illustrated correlation matrix (Fig. 8C). When ERS gene correlations with various immune cells were finally assessed (Fig. 8D), it was found that MBTPS2 considerably negatively correlated with both M1 macrophages and plasma cells, whereas QRICH1 significantly positively linked with M1 macrophages.

4. Discussion

Miscarriage stands as a common and intricate complication within human pathological reproduction [4]. Despite its high occurrence, effective clinical strategies to prevent RSA remain limited. Identifying novel and effective molecular targets for therapy becomes paramount. Numerous factors contribute to the pathogenesis of RSA, with increasing evidence highlighting the essential role of ERS in early pregnancy loss [9,37]. In this study, we performed a bioinformatics analysis to explore immunoinfiltration, developed a

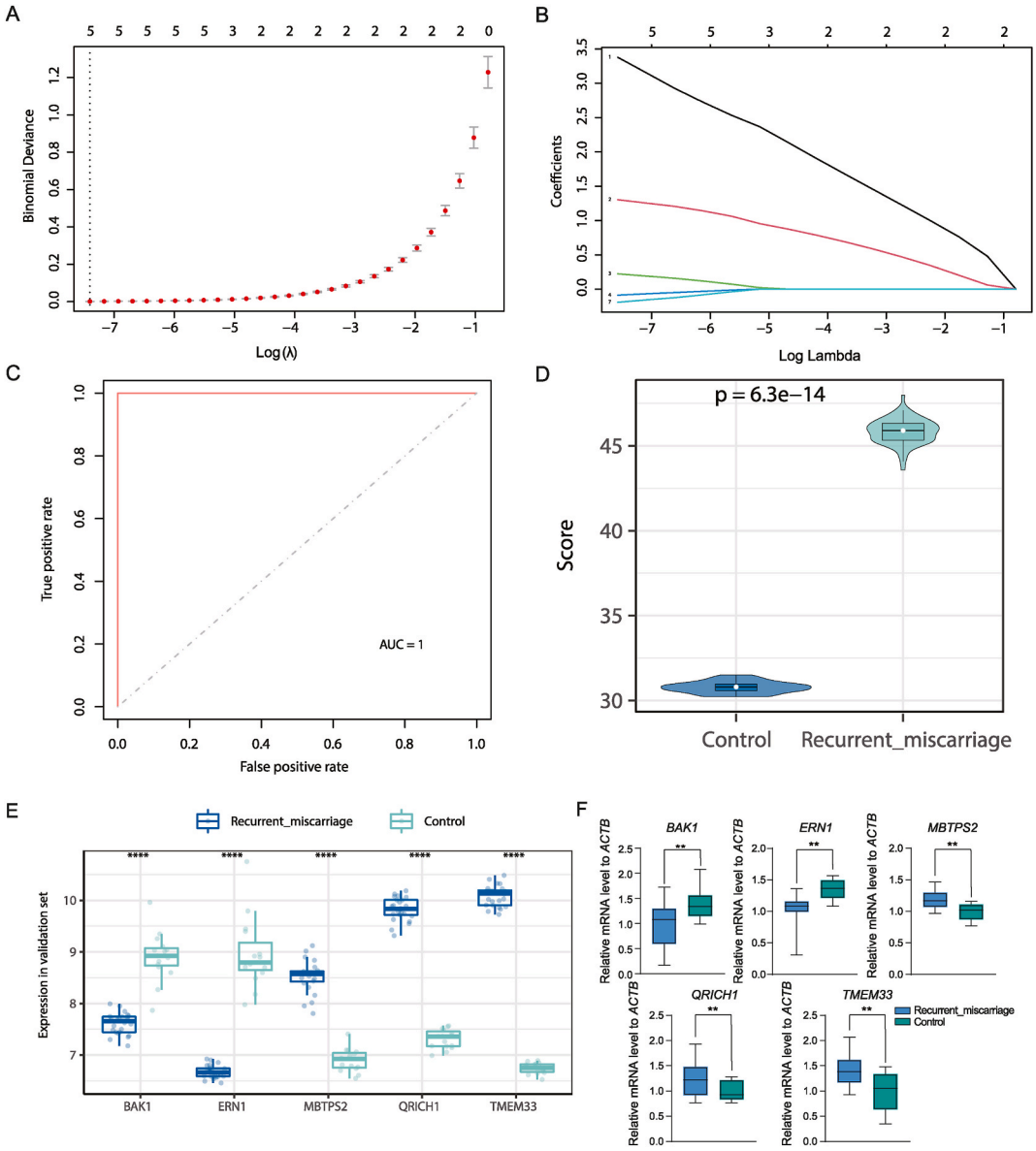

Fig. 4. Screening and validation of diagnostic markers. A-B. Utilization of LASSO regression to identify potential diagnostic markers, highlighting the partial likelihood deviance obtained from 10-fold cross-validation to establish the optimal lambda (λ) value. C. ROC curve analysis using LASSO regression to assess the diagnostic capability for RSA. D. Diagnostic scores in cases and controls. E. Evaluation of the expression profiles of five ERS markers in the validation dataset, comparing cases and controls to determine their diagnostic potential. F. Validation of the levels of ERS genes that are differentially expressed, with statistical comparisons conducted between cases and controls using the Wilcoxon test. $^{*}p < 0.05$, $^{**}p < 0.01$, $^{***}p < 0.001$, $^{****}p < 0.0001$.

competing endogenous RNA (ceRNA) network, and identified key genes related to ERS in RSA. Results point to ERS-related central genes like TMEM33, QRICH1, MBTPS2, ERN1, and BAK1 in association with RSA. Various immune cells, including macrophages, regulatory T cells, and dendritic cells, contribute to the RSA process [38–42]. This study enhances our comprehension of the function of ERS in RSA, suggesting these predicted genes as potential therapeutic targets or prognostic indicators.

Abnormal ERS contribute to the pathogenesis of RSA and immature development of endometrial decidualization [11,43,44]. Pathological endoplasmic reticulum stress indicates a disruption in endoplasmic reticulum homeostasis, with endoplasmic reticulum stress-induced suppression of the unfolded protein response (UPR) potentially impairing decidualization [45,46]. Therefore, exploring molecular therapeutic targets involved in RSA pathogenesis is essential for improving clinical outcomes in miscarriage prevention. In this work, we found 15 differently expressed ERS genes, including 6 upregulated and 9 downregulated.

TMEM33, a conserved transmembrane domain protein located on the nuclear membrane and ER, acts as a regulatory factor for tubular endoplasmic reticulum by inhibiting membrane-forming activity [47,48]. Recent studies have demonstrated TMEM33's

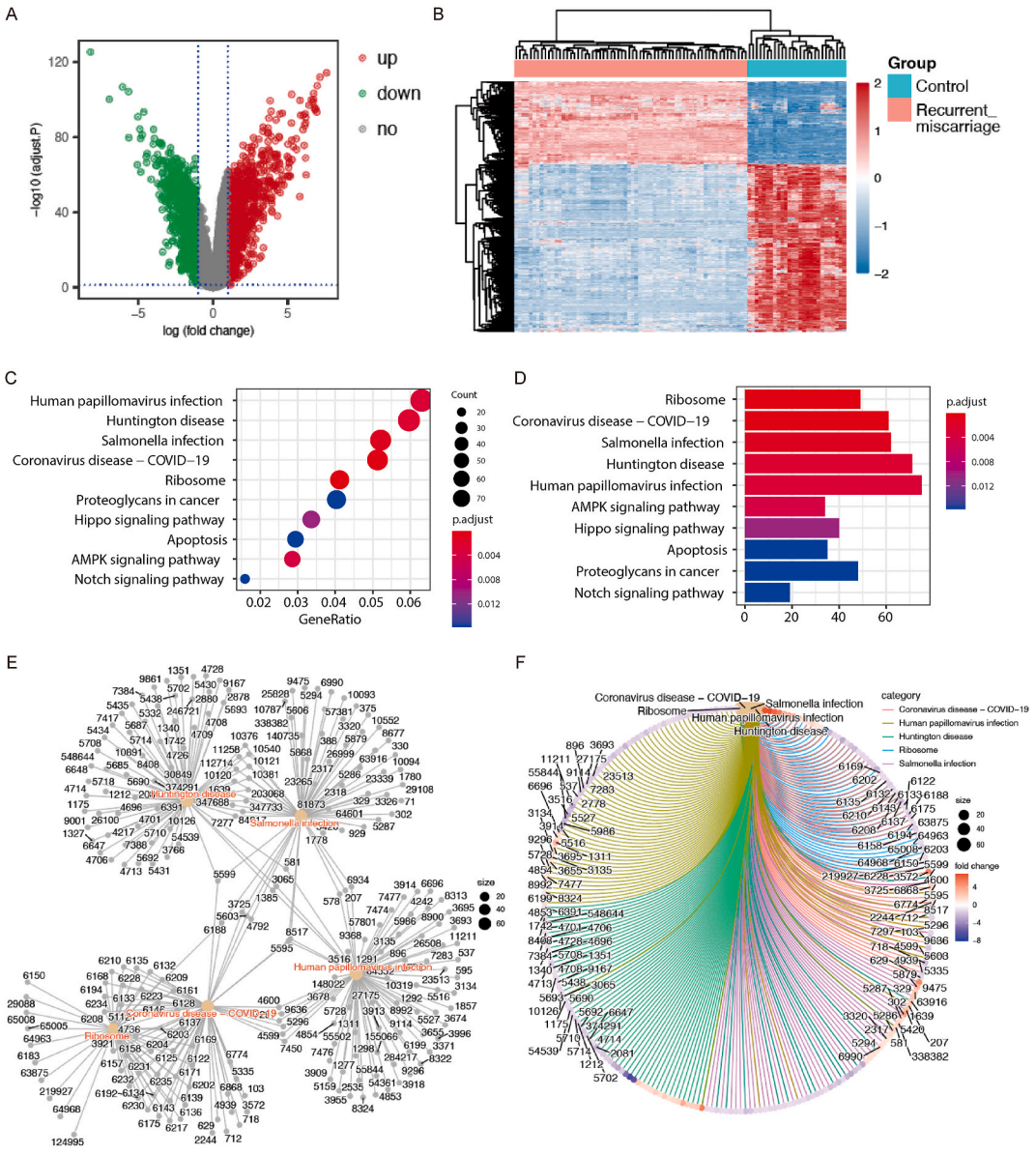

Fig. 5. Analysis of differentially expressed genes and KEGG pathway enrichment A. Volcano plot displaying the results of variance analysis, highlighting significant differentially expressed genes (DEGs) based on fold change and statistical significance. B. Heatmap displaying the results of the variance analysis, providing a visual representation of expression levels across samples for the identified DEGs. C. Bubble chart depicting the KEGG pathway enrichment analysis, where red bubbles indicate lower p-values, and larger bubbles represent pathways with a greater number of enriched DEGs. D. Bar chart presenting the KEGG pathway enrichment results, with the color red denoting smaller p-values. The X-axis represents the gene count associated with each pathway. E-F. Network diagrams illustrating the KEGG pathway results, showcasing the interconnections among enriched pathways and their associated DEGs.

diverse roles, including regulation of innate immune responses via the cGAS-STING pathway [47]. TMEM33 is also involved in EC-specific VEGF-mediated calcium oscillations [49], which promote vascular development in embryos [50]. Given that endometrial receptivity and pregnancy maintenance are influenced by immune responses and blood supply [51–55], the elevated expression of TMEM33 in our study suggests its potential role in RSA development, possibly affecting immune responses and blood supply. Further in vitro and in vivo investigations are warranted.

Additionally, previous research has linked RSA development to disruptions in various metabolic pathways. Our results validate correlations between miscarriages and abnormalities in the metabolism of alanine, aspartate, and glutamate, as well as taurine and hypotaurine, linoleic acid, and other substances [56–59]. Further evidence from our work supports the strong relationship between QRICH1 and the metabolism of taurine, hypotaurine, alanine, aspartate, and glutamate. Previous research has revealed QRICH1's function in ribosomal translation restart mechanisms and its significance as a major effector of the PERK-eIF2α axis in response to ER

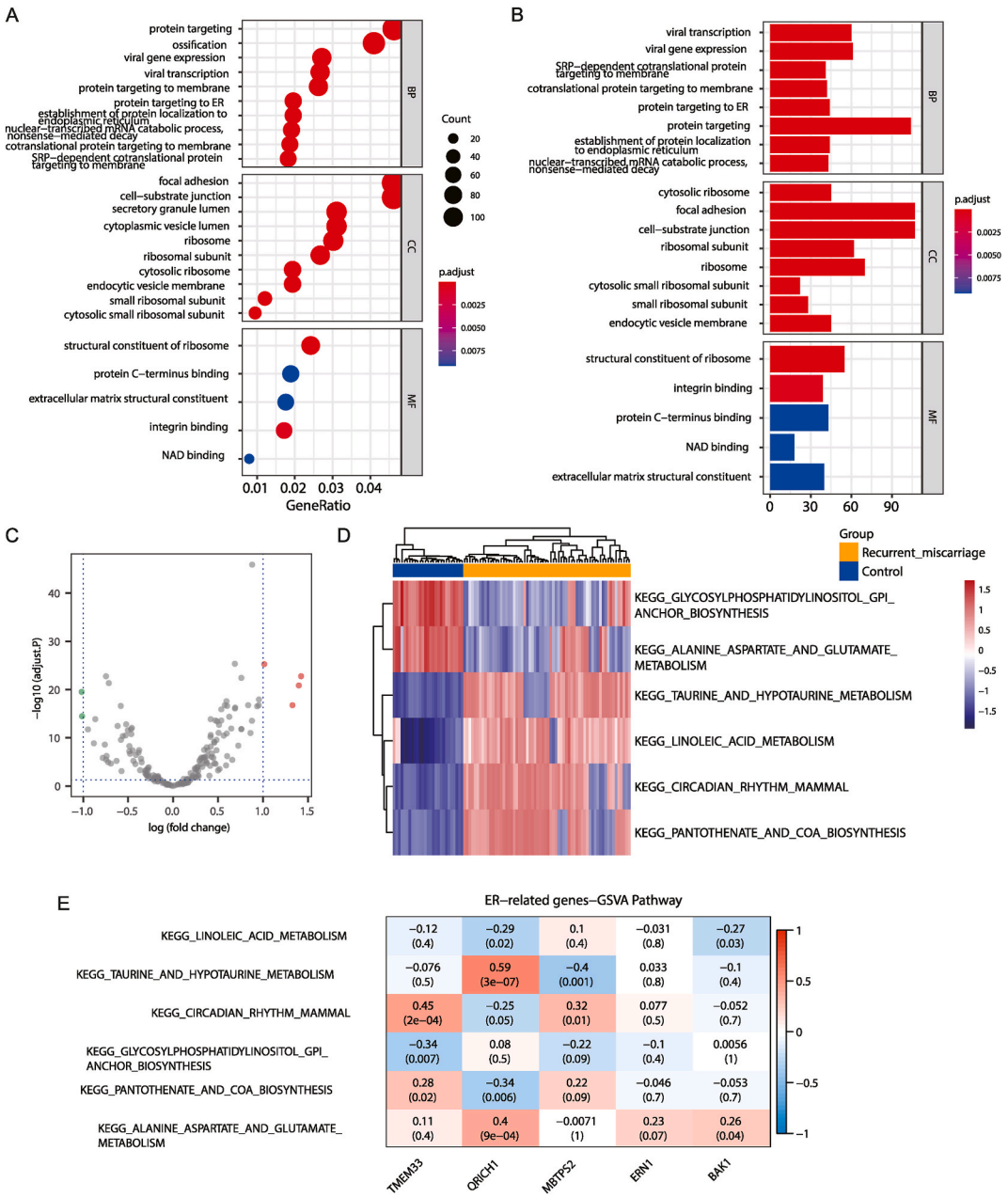

Fig. 6. GO and GSVA enrichment analysis. A. GO enrichment analysis outcomes for BP, CC, and MF, displayed as bubble charts. Red indicates a smaller p-value, and larger bubbles represent pathways enriched with more DEGs. B. GO enrichment results for BP, CC, and MF, displayed as bar charts, with red denoting smaller p-values. The X-axis represents the quantity of genes associated with each pathway. C. Volcano plot showcasing differential pathways identified through GSVA, with thresholds set at adjusted $p < 0.05$ and $|\log FC| > 1$, where green dots represent downregulated pathways. D. Heatmap showing enrichment scores of differential pathways between samples. E. Correlation matrix between differential pathways and ER gene expression levels. Red represents positive correlations, while blue signifies negative ones; darker shades signify stronger relationships. The matrix includes Pearson correlation coefficients and their corresponding p-values.

stress [60]. It follows that QRICH1 may have a role in both the metabolic pathophysiology of RSA and ER malfunction. Additionally, elevated levels of genes including MBTPS2, AGR2, NCK1, and BAX highlight the potential for further investigation into these genes and their signaling pathways to identify new treatment strategies for RSA.

We further delineated the regulatory molecular characteristics of differentially expressed ERS genes by creating distribution charts of transcription factors (TFs) and microRNAs (miRNAs) associated with each hub gene. Numerous novel TFs were found to bind to the promoters of several important regulators that were not previously examined and were involved in endometrial decidualization. Previous research has highlighted several TFs, such as KLF9, SP1, SP3, and FOXM1, which significantly impact disease progression

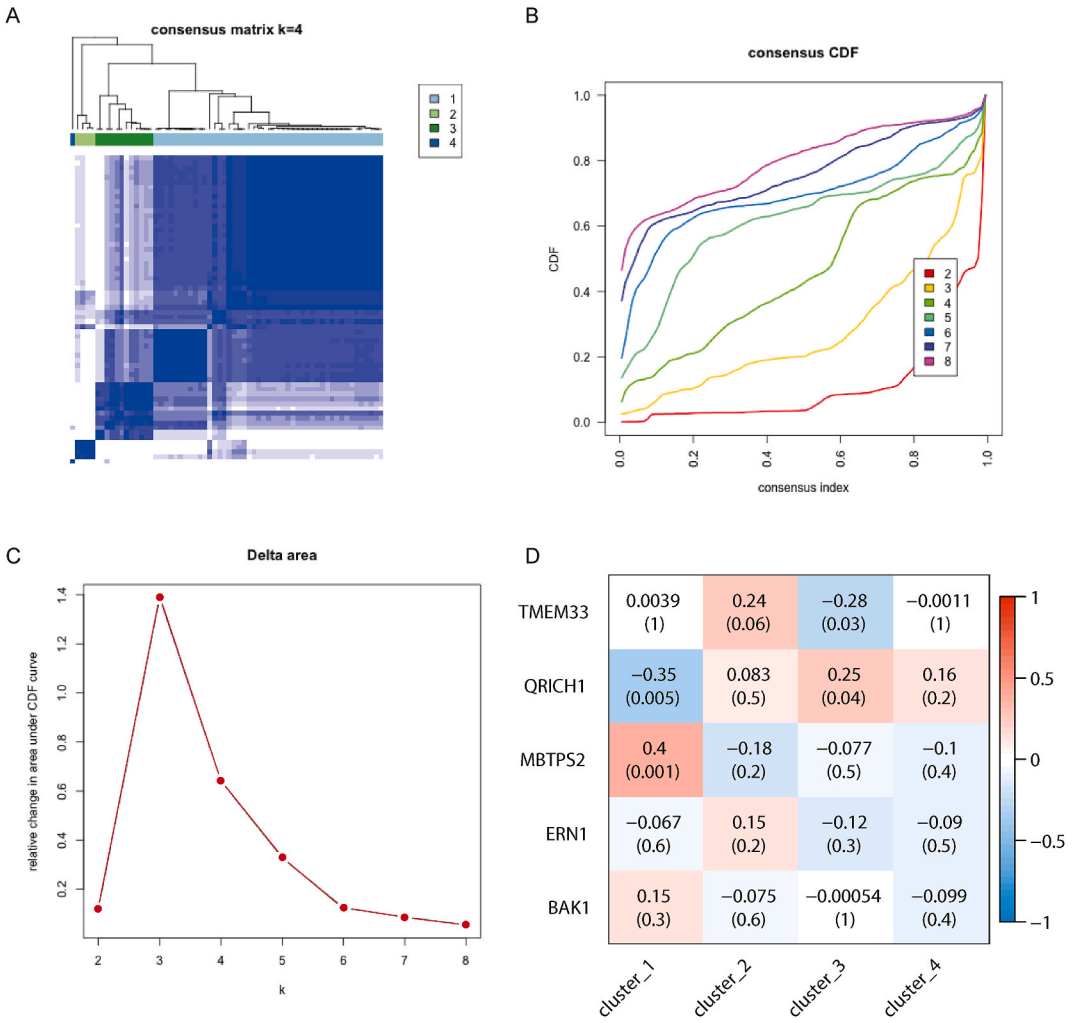

Fig. 7. Molecular subtype analysis. A-C. Construction of molecular subtypes. The increase in AUC of the CDF curve noticeably slowed when $K = 4$, which was selected for clustering. D. Correlation matrix between molecular subtype fractions and ER genes. Red represents positive correlations, while blue signifies negative ones; darker shades signify stronger relationships. The matrix includes Pearson correlation coefficients and their corresponding p-values.

[61–70]. We also conducted a thorough examination of the connections between the miRNA network and ERS-related genes (ERSRGs). Previous research has discovered that NF-κB is used by a number of microRNAs, including miR-155-5p, to control the survival of human decidual stromal cells in recurrent miscarriages [71,72]. Decidual natural killer cells' expression of miR-34a-3p is linked to URSA [73]. Lastly, we constructed a network of small molecules and compounds interacting with core target genes. This network facilitates the screening of affinities between compounds and gene targets, providing deeper insights into these relationships and aiding in the discovery of gene-targeted drugs and novel drug binding sites.

Numerous immune cells, including dendritic cells, Treg cells, and macrophages, are essential for regulating the immune response in RSA [38–40]. Immune cell infiltration can lead to an abundance of pro-inflammatory mediators, contributing to a cascade of inflammation within the placenta. Essential for human pregnancy, macrophages show notable adaptability in response to environmental cues, therefore controlling several reproductive processes including embryo implantation, placental development, fetal growth, and most importantly, vascular remodeling at the mother-fetal interface [74,75]. The polarization and functionality of macrophages, encompassing differentiation into M1 and M2 subtypes, are essential [38]. M1 macrophages are distinguished by elevated antigen presentation and pro-inflammatory responses, facilitating inflammation and tissue damage [76]. M1 macrophages exhibit elevated antigen presentation and pro-inflammatory reactions, whereas a balanced M1/M2 ratio is essential for successful pregnancy [77,78]. Disruption in this balance can lead to reproductive complications such as RSA, preeclampsia, and intrauterine growth restriction [79]. In our study, the RSA group exhibited significant macrophage infiltration, with QRICH1 among the ERSRGs showing a strong positive correlation with M1 macrophages. Consistent with our findings, other studies have linked macrophage infiltration, particularly M1 macrophages, to RSA development [74,80,81]. Furthermore, Treg cells and dendritic cells also play

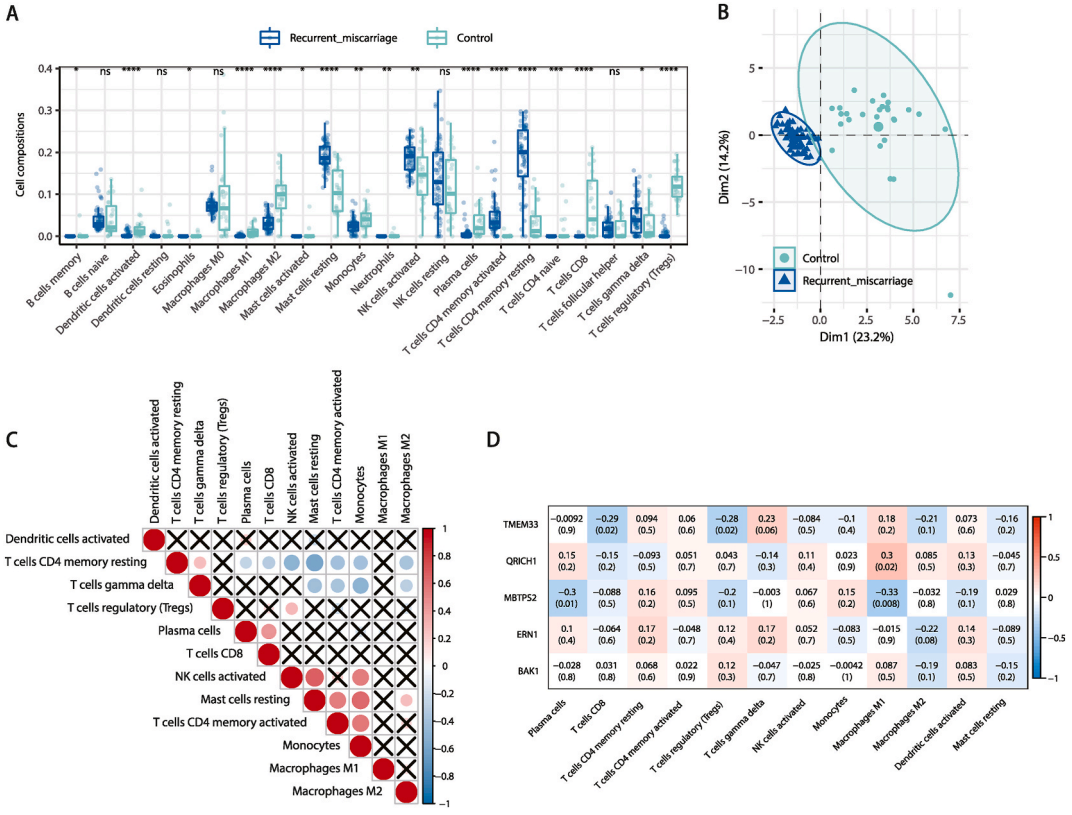

Fig. 8. Immune cell infiltration analysis. A. Comparison of immune cell infiltration levels between cases and controls, performed using the Wilcoxon test. $*p < 0.05$, $**p < 0.01$, $***p < 0.001$, $****p < 0.0001$. B. PCA plot illustrating the distribution of infiltrating immune cells across the sample groups. C. Correlation matrix depicting relationships among various immune cells; blue indicates positive correlations, red signifies negative correlations, and darker shades reflect stronger associations. Dark "X" marks represent correlations that are not statistically significant. D. Correlation matrix examining the relationships between immune cells and ERS genes; Red represents positive correlations, while blue signifies negative ones; and darker colors signify stronger correlations. Correlation coefficients and associated p-values are displayed within the matrix.

significant roles, suggesting that further research into the immune cell responses associated with ERS could lead to breakthroughs in RSA treatment.

At present, biotechnology is developing towards high-throughput, multi omics, and single-cell resolution. The single-cell sequencing and spatial transcriptomics have been developed. These technologies provide more comprehensive, efficient, and in-depth research methods for biological research, overcoming the drawbacks of traditional biological research methods. Single cell sequencing is a new technology formed by combining single-cell technology with high-throughput sequencing technology. The main difficulty and difference between it and traditional sequencing lies in the pre-processing before sequencing, including single-cell capture, target DNA/RNA extraction, weak signal amplification (i.e. amplifying a very small number of DNA strands), etc [82,83]. Spatial transcriptome analysis is the use of probes with spatial barcodes to sequence slices. Combined with ScRNA seq, it can map cell subpopulations obtained from high-resolution single-cell data to space, and infer the functions and differentiation relationships of different subpopulations [84]. The multi-omics is composed of multiple technologies. In the future, we have the capacity to conduct more exhaustive and in-depth research on recurrent miscarriage. Based on this work, our next plan is to use multi omics techniques to further study recurrent miscarriage, hoping to gain a more comprehensive and in-depth understanding [82].

While bioinformatics methods offer valuable insights into the molecular mechanisms underlying RSA, this study acknowledges certain limitations. Although bioinformatics provides rich information on biomarkers, there is insufficient evidence to seamlessly link all database data with gestational outcomes. Future work will focus on integrating minimally invasive or non-invasive bioinformatics tools and developing a more comprehensive interpretation of data to address challenges in clinical application. Validation of our findings requires additional cohorts with substantial sample sizes and basic experimental expertise. Further validation through protein imprinting, immunohistochemistry, and immunofluorescence assays is necessary to confirm the differential expression of ERS genes identified in our analysis. Additionally, it is critical to use gain-of-function and loss-of-function experiments to investigate the functional features of ERS genes expression at the cellular and tissue-specific levels. Ultimately, prospective clinical studies are essential for translating identified biomarkers into clinical practice, representing potential avenues for future research.

5. Conclusion

To sum up, this research offers a thorough investigation of the molecular mechanisms behind RSA by means of comprehensive bioinformatics studies. We examined the roles and enriched pathways of five crucial genes that were found to be intimately connected with RSA-associated ERS. Our all-encompassing bioinformatics method also identified the important regulatory processes, immune infiltration traits, and ceRNA network implicated in RSA. To our knowledge, our work marks the establishment of a comprehensive regulatory network for core genes related to ERS, shedding light on the biological mechanisms of RSA. Our results open up new avenues for investigation into the involvement of immune cell responses and ERS genes in RSA, which may result in novel approaches to diagnosis and treatment for those with RSA difficulties.

Ethics approval

This study received comprehensive ethical oversight and approval from the Research Ethics Committee of the Seventh Affiliated Hospital of Sun Yat-sen University, reference number KY-2021-044-01, on April 20, 2021, after an extensive evaluation of the study's protocols and methodologies to ensure adherence to ethical standards. Prior to engaging in the investigation, each participant executed informed consent.

Funding

The National Natural Science Foundation of China (NSFC, Grant Nos. 82000150 and 82202579) provided funding for this work.

Data availability

The study's original data have been added to a repository that is open to the public. The sequencing data used in this work were specifically deposited in GEO with accession codes GSE77688 and GSE141549. The data processing steps are available in the publication [and/or] its additional materials, as confirmed by the authors.

CRediT authorship contribution statement

Tao Tang: Writing – original draft, Investigation, Data curation, Conceptualization. **Jingyu Fu:** Writing – original draft, Data curation, Conceptualization. **Chong Zhang:** Writing – original draft, Data curation, Conceptualization. **Xue Wang:** Visualization, Methodology, Formal analysis. **Haiming Cao:** Writing – review & editing, Supervision, Resources, Project administration, Funding acquisition. **Lin Chen:** Writing – review & editing, Supervision, Resources, Project administration, Funding acquisition, Conceptualization.

Declaration of competing interest

The authors declare the following financial interests/personal relationships which may be considered as potential competing interests:Lin Chen reports financial support was provided by National Natural Science Foundation of China. If there are other authors, they declare that they have no known competing financial interests or personal relationships that could have appeared to influence the work reported in this paper.

Acknowledgements

Not applicable.

Appendix A. Supplementary data

Supplementary data to this article can be found online at https://doi.org/10.1016/j.heliyon.2024.e38964.

References

[1] T. Laisk, A.L.G. Soares, T. Ferreira, J.N. Painter, et al., The genetic architecture of sporadic and multiple consecutive miscarriage, Nat. Commun. 11 (2020) 5980, https://doi.org/10.1038/s41467-020-19742-5.
[2] a. a. o. Practice Committee of the American Society for Reproductive Medicine, Electronic address, Definitions of infertility and recurrent pregnancy loss: a committee opinion, Fertil. Steril. 113 (2020) 533–535, https://doi.org/10.1016/j.fertnstert.2019.11.025.
[3] L. Marozio, A.M. Nuzzo, E. Gullo, L. Moretti, et al., Immune checkpoints in recurrent pregnancy loss: new insights into a detrimental and elusive disorder, Int. J. Mol. Sci. 24 (2023), https://doi.org/10.3390/ijms241713071.
[4] E. Dimitriadis, E. Menkhorst, S. Saito, W.H. Kutteh, et al., Recurrent pregnancy loss, Nat. Rev. Dis. Prim. 6 (2020) 98, https://doi.org/10.1038/s41572-020-00228-z.

[5] S.A. Oakes, F.R. Papa, The role of endoplasmic reticulum stress in human pathology, Annu. Rev. Pathol. 10 (2015) 173–194, https://doi.org/10.1146/annurev-pathol-012513-104649.
[6] H.P. Harding, I. Novoa, Y. Zhang, H. Zeng, et al., Regulated translation initiation controls stress-induced gene expression in mammalian cells, Mol. Cell 6 (2000) 1099–1108, https://doi.org/10.1016/s1097-2765(00)00108-8.
[7] Y. Ergun, A.G. Imamoglu, M. Cozzolino, C. Demirkiran, et al., Mitochondrial unfolded protein response gene Clpp is required for oocyte function and female fertility, Int. J. Mol. Sci. 25 (2024), https://doi.org/10.3390/ijms25031866.
[8] E. Sung, W. Park, J. Park, F.W. Bazer, et al., Meptyldinocap induces implantation failure by forcing cell cycle arrest, mitochondrial dysfunction, and endoplasmic reticulum stress in porcine trophectoderm and endometrial luminal epithelial cells, Sci. Total Environ. 924 (2024) 171524, https://doi.org/10.1016/j.scitotenv.2024.171524.
[9] T. Lin, J.E. Lee, J.W. Kang, H.Y. Shin, et al., Endoplasmic reticulum (ER) stress and unfolded protein response (UPR) in mammalian oocyte maturation and preimplantation embryo development, Int. J. Mol. Sci. 20 (2019), https://doi.org/10.3390/ijms20020409.
[10] X. Tang, Y. Geng, R. Gao, Z. Chen, et al., Maternal exposure to beta-Cypermethrin disrupts placental development by dysfunction of trophoblast cells from oxidative stress, Toxicology 504 (2024) 153796, https://doi.org/10.1016/j.tox.2024.153796.
[11] Y. Tang, X. Zhang, Y. Zhang, H. Feng, et al., Senescent changes and endoplasmic reticulum stress may Be involved in the pathogenesis of missed miscarriage, Front. Cell Dev. Biol. 9 (2021) 656549, https://doi.org/10.3389/fcell.2021.656549.
[12] C. Xu, B. Bailly-Maitre, J.C. Reed, Endoplasmic reticulum stress: cell life and death decisions, J. Clin. Invest. 115 (2005) 2656–2664, https://doi.org/10.1172/JCI26373.
[13] H. Koike, M. Harada, A. Kusamoto, Z. Xu, et al., Roles of endoplasmic reticulum stress in the pathophysiology of polycystic ovary syndrome, Front. Endocrinol. 14 (2023) 1124405, https://doi.org/10.3389/fendo.2023.1124405.
[14] J. Ham, W. Park, J. Song, H.S. Kim, et al., Fraxetin reduces endometriotic lesions through activation of ER stress, induction of mitochondria-mediated apoptosis, and generation of ROS, Phytomedicine 123 (2024) 155187, https://doi.org/10.1016/j.phymed.2023.155187.
[15] B. Cao, A.J. Camden, L.A. Parnell, I.U. Mysorekar, Autophagy regulation of physiological and pathological processes in the female reproductive tract, Am. J. Reprod. Immunol. 77 (2017), https://doi.org/10.1111/aji.12650.
[16] S.E. Ander, M.S. Diamond, C.B. Coyne, Immune responses at the maternal-fetal interface, Sci Immunol 4 (2019), https://doi.org/10.1126/sciimmunol.aat6114.
[17] H. Dong, N.M. Adams, Y. Xu, J. Cao, et al., The IRE1 endoplasmic reticulum stress sensor activates natural killer cell immunity in part by regulating c-Myc, Nat. Immunol. 20 (2019) 865–878, https://doi.org/10.1038/s41590-019-0388-z.
[18] T. Yue, Y. Guo, X. Qi, W. Zheng, et al., Sex-biased regulatory changes in the placenta of native highlanders contribute to adaptive fetal development, Elife 12 (2024), https://doi.org/10.7554/eLife.89004.
[19] Y. Yao, Y. Ye, J. Chen, M. Zhang, et al., Maternal-fetal immunity and recurrent spontaneous abortion, Am. J. Reprod. Immunol. 91 (2024) e13859, https://doi.org/10.1111/aji.13859.
[20] L. Li, Z. Zhang, H. Li, M. Zhou, et al., Research progress on the STAT signaling pathway in pregnancy and pregnancy-associated disorders, Front. Immunol. 14 (2023) 1331964, https://doi.org/10.3389/fimmu.2023.1331964.
[21] Q.H. Li, Q.Y. Zhao, W.J. Yang, A.F. Jiang, et al., Beyond immune balance: the pivotal role of decidual regulatory T cells in unexplained recurrent spontaneous abortion, J. Inflamm. Res. 17 (2024) 2697–2710, https://doi.org/10.2147/jir.S459263.
[22] C. Garrido-Gimenez, J. Alijotas-Reig, Recurrent miscarriage: causes, evaluation and management, Postgrad. Med. 91 (2015) 151–162, https://doi.org/10.1136/postgradmedj-2014-132672.
[23] J.T. Leek, W.E. Johnson, H.S. Parker, A.E. Jaffe, et al., The sva package for removing batch effects and other unwanted variation in high-throughput experiments, Bioinformatics 28 (2012) 882–883, https://doi.org/10.1093/bioinformatics/bts034.
[24] G.K. Smyth, Linear models and empirical bayes methods for assessing differential expression in microarray experiments, Stat. Appl. Genet. Mol. Biol. 3 (2004) Article3, https://doi.org/10.2202/1544-6115.1027.
[25] E.K. Gustavsson, D. Zhang, R.H. Reynolds, S. Garcia-Ruiz, et al., ggtranscript: an R package for the visualization and interpretation of transcript isoforms using ggplot2, Bioinformatics 38 (2022) 3844–3846, https://doi.org/10.1093/bioinformatics/btac409.
[26] D. Szklarczyk, A.L. Gable, D. Lyon, A. Junge, et al., STRING v11: protein-protein association networks with increased coverage, supporting functional discovery in genome-wide experimental datasets, Nucleic Acids Res. 47 (2019) D607–D613, https://doi.org/10.1093/nar/gky1131.
[27] D. Otasek, J.H. Morris, J. Boucas, A.R. Pico, et al., Cytoscape Automation: empowering workflow-based network analysis, Genome Biol. 20 (2019) 185, https://doi.org/10.1186/s13059-019-1758-4.
[28] J. Xia, E.E. Gill, R.E. Hancock, NetworkAnalyst for statistical, visual and network-based meta-analysis of gene expression data, Nat. Protoc. 10 (2015) 823–844, https://doi.org/10.1038/nprot.2015.052.
[29] Y. Xie, H. Shi, B. Han, Bioinformatic analysis of underlying mechanisms of Kawasaki disease via weighted gene correlation network analysis (WGCNA) and the least absolute shrinkage and selection operator method (LASSO) regression model, BMC Pediatr. 23 (2023) 90, https://doi.org/10.1186/s12887-023-03896-4.
[30] A.J. McEligot, V. Poynor, R. Sharma, A. Panangadan, Logistic LASSO regression for dietary intakes and breast cancer, Nutrients 12 (2020), https://doi.org/10.3390/nu12092652.
[31] S. Engebretsen, J. Bohlin, Statistical predictions with glmnet, Clin. Epigenet. 11 (2019) 123, https://doi.org/10.1186/s13148-019-0730-1.
[32] G. Yu, L.G. Wang, Y. Han, Q.Y. He, clusterProfiler: an R Package for Comparing Biological Themes Among Gene Clusters, vol. 16, OMICS, 2012, pp. 284–287, https://doi.org/10.1089/omi.2011.0118.
[33] Gene Ontology Consortium: going forward, Nucleic Acids Res. 43 (2015) D1049–D1056, https://doi.org/10.1093/nar/gku1179.
[34] J. Du, Z. Yuan, Z. Ma, J. Song, et al., KEGG-PATH: Kyoto encyclopedia of genes and genomes-based pathway analysis using a path analysis model, Mol. Biosyst. 10 (2014) 2441–2447, https://doi.org/10.1039/c4mb00287c.
[35] S. Hanzelmann, R. Castelo, J. Guinney, GSVA: gene set variation analysis for microarray and RNA-seq data, BMC Bioinf. 14 (2013) 7, https://doi.org/10.1186/1471-2105-14-7.
[36] M.D. Wilkerson, D.N. Hayes, ConsensusClusterPlus: a class discovery tool with confidence assessments and item tracking, Bioinformatics 26 (2010) 1572–1573, https://doi.org/10.1093/bioinformatics/btq170.
[37] N.F. Topbas Selcuki, P. Yalcin Bahat, N. Deniz, C. Kaya, et al., Relationship between recurrent pregnancy loss with unknown etiology and endoplasmic reticulum stress, Cureus 16 (2024) e60899, https://doi.org/10.7759/cureus.60899.
[38] Y. Yao, X.H. Xu, L. Jin, Macrophage polarization in physiological and pathological pregnancy, Front. Immunol. 10 (2019) 792, https://doi.org/10.3389/fimmu.2019.00792.
[39] W. Wang, N. Sung, A. Gilman-Sachs, J. Kwak-Kim, T helper (Th) cell profiles in pregnancy and recurrent pregnancy losses: Th1/Th2/Th9/Th17/Th22/Tfh cells, Front. Immunol. 11 (2020) 2025, https://doi.org/10.3389/fimmu.2020.02025.
[40] R. Wei, N. Lai, L. Zhao, Z. Zhang, et al., Dendritic cells in pregnancy and pregnancy-associated diseases, Biomed. Pharmacother. 133 (2021) 110921, https://doi.org/10.1016/j.biopha.2020.110921.
[41] C. Tang, W. Hu, Non-coding RNA regulates the immune microenvironment in recurrent spontaneous abortion (RSA): new insights into immune mechanisms, Biol. Reprod. 110 (2024) 220–229, https://doi.org/10.1093/biolre/ioad157.
[42] M. Andreescu, F. Frîncu, M. Plotogea, C. Mehedințu, Recurrent abortion and the involvement of killer-cell immunoglobulin-like receptor (KIR) genes, activated T cells, NK abnormalities, and cytokine profiles, J. Clin. Med. 12 (2023), https://doi.org/10.3390/jcm12041355.
[43] M.H. Pan, K.H. Zhang, S.L. Wu, Z.N. Pan, et al., FMNL2 regulates actin for endoplasmic reticulum and mitochondria distribution in oocyte meiosis, Elife 12 (2024), https://doi.org/10.7554/eLife.92732.
[44] T. Hong, S. Park, G. An, F.W. Bazer, et al., Norflurazon causes cell death and inhibits implantation-related genes in porcine trophectoderm and uterine luminal epithelial cells, Food Chem. Toxicol. 186 (2024) 114559, https://doi.org/10.1016/j.fct.2024.114559.

[45] K. Yoshida, K. Kusama, M. Azumi, M. Yoshie, et al., Endoplasmic reticulum stress-regulated high temperature requirement A1 (HTRA1) modulates invasion and angiogenesis-related genes in human trophoblasts, J. Pharmacol. Sci. 150 (2022) 267–274, https://doi.org/10.1016/j.jphs.2022.10.003.
[46] E. Soczewski, J.M. Murrieta-Coxca, L. Miranda, P. Fuentes-Zacarías, et al., miRNAs associated with endoplasmic reticulum stress and unfolded protein response during decidualization, Reprod. Biomed. Online 47 (2023) 103289, https://doi.org/10.1016/j.rbmo.2023.103289.
[47] E.J. Fenech, F. Lari, P.D. Charles, R. Fischer, et al., Interaction mapping of endoplasmic reticulum ubiquitin ligases identifies modulators of innate immune signalling, Elife 9 (2020), https://doi.org/10.7554/eLife.57306.
[48] M. Kamil, U.Y. Kina, H.N. Atmaca, S. Unal, et al., Endoplasmic reticulum localized TMEM33 domain-containing protein is crucial for all life cycle stages of the malaria parasite, Mol. Microbiol. 121 (2024) 767–780, https://doi.org/10.1111/mmi.15228.
[49] M. Arhatte, G.S. Gunaratne, C. El Boustany, I.Y. Kuo, et al., TMEM33 regulates intracellular calcium homeostasis in renal tubular epithelial cells, Nat. Commun. 10 (2019) 2024, https://doi.org/10.1038/s41467-019-10045-y.
[50] A.M. Savage, S. Kurusamy, Y. Chen, Z. Jiang, et al., tmem33 is essential for VEGF-mediated endothelial calcium oscillations and angiogenesis, Nat. Commun. 10 (2019) 732, https://doi.org/10.1038/s41467-019-08590-7.
[51] W. Cowell, N. Ard, T. Herrera, E.A. Medley, et al., Ambient temperature, heat stress and fetal growth: a review of placenta-mediated mechanisms, Mol. Cell. Endocrinol. 576 (2023) 112000, https://doi.org/10.1016/j.mce.2023.112000.
[52] F. Yang, Q. Zheng, L. Jin, Dynamic function and composition changes of immune cells during normal and pathological pregnancy at the maternal-fetal interface, Front. Immunol. 10 (2019) 2317, https://doi.org/10.3389/fimmu.2019.02317.
[53] B. Abu-Raya, C. Michalski, M. Sadarangani, P.M. Lavoie, Maternal immunological adaptation during normal pregnancy, Front. Immunol. 11 (2020) 575197, https://doi.org/10.3389/fimmu.2020.575197.
[54] J.D. Aplin, J.E. Myers, K. Timms, M. Westwood, Tracking placental development in health and disease, Nat. Rev. Endocrinol. 16 (2020) 479–494, https://doi.org/10.1038/s41574-020-0372-6.
[55] P. Artimovič, Z. Badovská, S. Toporcerová, I. Špaková, et al., Oxidative stress and the Nrf2/PPARγ Axis in the endometrium: insights into female fertility, Cells 13 (2024), https://doi.org/10.3390/cells13131081.
[56] T. Hussain, B. Tan, G. Murtaza, E. Metwally, et al., Role of dietary amino acids and nutrient sensing system in pregnancy associated disorders, Front. Pharmacol. 11 (2020) 586979, https://doi.org/10.3389/fphar.2020.586979.
[57] M. Szczuko, J. Kikut, N. Komorniak, J. Bilicki, et al., The role of arachidonic and linoleic acid derivatives in pathological pregnancies and the human reproduction process, Int. J. Mol. Sci. 21 (2020), https://doi.org/10.3390/ijms21249628.
[58] L. Li, N. Ning, J.A. Wei, Q.L. Huang, et al., Metabonomics study on the infertility treated with Zishen Yutai pills combined with in vitro fertilization-embryo transfer, Front. Pharmacol. 12 (2021) 686133, https://doi.org/10.3389/fphar.2021.686133.
[59] Y. Zhang, T. Zhang, L. Wu, T.C. Li, et al., Metabolomic markers of biological fluid in women with reproductive failure: a systematic review of current literatures, Biol. Reprod. 106 (2022) 1049–1058, https://doi.org/10.1093/biolre/ioac038.
[60] K. You, L. Wang, C.H. Chou, K. Liu, et al., QRICH1 dictates the outcome of ER stress through transcriptional control of proteostasis, Science 371 (2021), https://doi.org/10.1126/science.abb6896.
[61] M.E. Heard, J.M. Pabona, C. Clayberger, A.M. Krensky, et al., The reproductive phenotype of mice null for transcription factor Krüppel-like factor 13 suggests compensatory function of family member Krüppel-like factor 9 in the peri-implantation uterus, Biol. Reprod. 87 (2012) 115, https://doi.org/10.1095/biolreprod.112.102251.
[62] E. Grasso, S. Gori, D. Paparini, E. Soczewski, et al., VIP induces the decidualization program and conditions the immunoregulation of the implantation process, Mol. Cell. Endocrinol. 460 (2018) 63–72, https://doi.org/10.1016/j.mce.2017.07.006.
[63] J.M. Pabona, Z. Zeng, F.A. Simmen, R.C. Simmen, Functional differentiation of uterine stromal cells involves cross-regulation between bone morphogenetic protein 2 and Kruppel-like factor (KLF) family members KLF9 and KLF13, Endocrinology 151 (2010) 3396–3406, https://doi.org/10.1210/en.2009-1370.
[64] F. Tian, Y. Zhang, J. Li, Z. Chu, et al., Effects of the SPI/lncRNA NEAT1 Axis on functions of trophoblast and decidual cells in patients with recurrent miscarriage, Crit. Rev. Eukaryot. Gene Expr. 33 (2023) 47–60, https://doi.org/10.1615/CritRevEukaryotGeneExpr.2022045376.
[65] H. Tang, L. Pan, Y. Xiong, L. Wang, et al., Down-regulation of the Sp1 transcription factor by an increase of microRNA-4497 in human placenta is associated with early recurrent miscarriage, Reprod. Biol. Endocrinol. 19 (2021) 21, https://doi.org/10.1186/s12958-021-00701-8.
[66] M. Tang, J. Mazella, J. Gao, L. Tseng, Progesterone receptor activates its promoter activity in human endometrial stromal cells, Mol. Cell. Endocrinol. 192 (2002) 45–53, https://doi.org/10.1016/s0303-7207(02)00111-9.
[67] J. Cui, X. Liu, L. Yang, S. Che, et al., MiR-184 combined with STC2 promotes endometrial epithelial cell apoptosis in dairy goats via RAS/RAF/MEK/ERK pathway, Genes 11 (2020), https://doi.org/10.3390/genes11091052.
[68] Y. Jiang, Y. Liao, H. He, Q. Xin, et al., FoxM1 directs STAT3 expression essential for human endometrial stromal decidualization, Sci. Rep. 5 (2015) 13735, https://doi.org/10.1038/srep13735.
[69] Y. Wang, X. Zhao, Z. Li, W. Wang, et al., Decidual natural killer cells dysfunction is caused by IDO downregulation in dMDSCs with Toxoplasma gondii infection, Commun. Biol. 7 (2024) 669, https://doi.org/10.1038/s42003-024-06365-5.
[70] M. Zhou, Y. Gao, S. Wu, Y. Wang, et al., USP22 is required for human endometrial stromal cell proliferation and decidualization by deubiquitinating FoxM1, Cell. Signal. 121 (2024) 111265, https://doi.org/10.1016/j.cellsig.2024.111265.
[71] Q. Zhang, P. Tian, H. Xu, MicroRNA-155-5p regulates survival of human decidua stromal cells through NF-κB in recurrent miscarriage, Reprod. Biol. 21 (2021) 100510, https://doi.org/10.1016/j.repbio.2021.100510.
[72] C. Guo, X. Yin, S. Yao, The effect of MicroRNAs variants on idiopathic recurrent pregnancy loss, J. Assist. Reprod. Genet. 40 (2023) 1589–1595, https://doi.org/10.1007/s10815-023-02827-7.
[73] D. Li, J. Li, Association of miR-34a-3p/5p, miR-141-3p/5p, and miR-24 in decidual natural killer cells with unexplained recurrent spontaneous abortion, Med Sci Monit 22 (2016) 922–929, https://doi.org/10.12659/msm.895459.
[74] Q.Y. Zhao, Q.H. Li, Y.Y. Fu, C.E. Ren, et al., Decidual macrophages in recurrent spontaneous abortion, Front. Immunol. 13 (2022) 994888, https://doi.org/10.3389/fimmu.2022.994888.
[75] H. True, M. Blanton, S. Sureshchandra, I. Messaoudi, Monocytes and macrophages in pregnancy: the good, the bad, and the ugly, Immunol. Rev. 308 (2022) 77–92, https://doi.org/10.1111/imr.13080.
[76] L. Wang, H. Wang, J. Luo, T. Xie, et al., Decorin promotes decidual M1-like macrophage polarization via mitochondrial dysfunction resulting in recurrent pregnancy loss, Theranostics 12 (2022) 7216–7236, https://doi.org/10.7150/thno.78467.
[77] C. Ticconi, A. Pietropolli, N. Di Simone, E. Piccione, et al., Endometrial immune dysfunction in recurrent pregnancy loss, Int. J. Mol. Sci. 20 (2019), https://doi.org/10.3390/ijms20215332.
[78] J. Feng, P. Gao, T. Wu, W. Hou, et al., Imbalance polarization of M1/M2 macrophages in miscarried uterus, PLoS One 19 (2024) e0304590, https://doi.org/10.1371/journal.pone.0304590.
[79] F. Sun, S. Wang, M. Du, Functional regulation of decidual macrophages during pregnancy, J. Reprod. Immunol. 143 (2021) 103264, https://doi.org/10.1016/j.jri.2020.103264.
[80] J. Ding, Y. Zhang, X. Cai, Y. Zhang, et al., Extracellular vesicles derived from M1 macrophages deliver miR-146a-5p and miR-146b-5p to suppress trophoblast migration and invasion by targeting TRAF6 in recurrent spontaneous abortion, Theranostics 11 (2021) 5813–5830, https://doi.org/10.7150/thno.58731.
[81] X. Chen, Q.L. Song, R. Ji, J.Y. Wang, et al., JPT2 affects trophoblast functions and macrophage polarization and metabolism, and acts as a potential therapeutic target for recurrent spontaneous abortion, Adv. Sci. 11 (2024) e2306359, https://doi.org/10.1002/advs.202306359.

[82] S. Bao, Z. Chen, D. Qin, H. Xu, et al., Single-cell profiling reveals mechanisms of uncontrolled inflammation and glycolysis in decidual stromal cell subtypes in recurrent miscarriage, Hum. Reprod. 38 (2023) 57–74, https://doi.org/10.1093/humrep/deac240.
[83] A. Tanay, A. Regev, Scaling single-cell genomics from phenomenology to mechanism, Nature 541 (2017) 331–338, https://doi.org/10.1038/nature21350.
[84] P.L. Ståhl, F. Salmén, S. Vickovic, A. Lundmark, et al., Visualization and analysis of gene expression in tissue sections by spatial transcriptomics, Science 353 (2016) 78–82, https://doi.org/10.1126/science.aaf2403.